



Contents lists available at ScienceDirect

Earth and Planetary Science Letters

www.elsevier.com/locate/epsl



In situ confirmation of permeability development in shearing bubble-bearing melts and implications for volcanic outgassing

Alexandra R.L. Kushnir*, Caroline Martel, Rémi Champallier, Laurent Arbaret

Institut des Sciences de la Terre d'Orléans (ISTO), UMR 7327 – CNRS/Université d'Orléans/BRGM, 1A, Rue de la Fêrolierie, 45071 Orléans Cedex 2, France

ARTICLE INFO

Article history:

Received 5 July 2016

Received in revised form 25 October 2016

Accepted 25 October 2016

Available online xxx

Editor: T.A. Mather

Keywords:

Mode I fractures

torsion

magma

outgassing

experiments

ABSTRACT

The ferocity of volcanic eruptions – their penchant for either effusive or explosive behaviour – is to a large extent a matter of the ease with which volatiles are able to escape the volcanic system. Of particular importance are the mechanisms by which permeable networks within magma are fabricated and how they permit gas escape, thereby diffusing possibly calamitous explosions. Here, we present a series of experiments that confirms sample-scale fracture propagation and permeability development during shearing viscous flow of initially impermeable, bubble-bearing (<0.20 bubble fraction) magmas under conditions pertinent to volcanic conduits. These samples are deformed in torsion at constant shear strain rates until an applied differential pore fluid pressure across the sample equilibrates, confirming permeability development *in situ*. Permeability develops at moderate to high shear strain rates ($\dot{\gamma} > 2 \times 10^{-4} \text{ s}^{-1}$). At moderate shear strain rates ($2 \times 10^{-4} \text{ s}^{-1} < \dot{\gamma} < 4.5 \times 10^{-4} \text{ s}^{-1}$), permeability initiates at high strain ($\gamma > 3$) via en échelon Mode I fractures produced by repeated fracture events. At high shear strain rates ($\dot{\gamma} > 4.5 \times 10^{-4} \text{ s}^{-1}$), permeability develops shortly after the onset of inelastic deformation and is, again, established through a series of en échelon Mode I fractures. Critically, strain is not immediately localized on Mode I fractures, making them long-lived and efficient outgassing channels that are ideally oriented for directing volatiles from the central conduit upward and outward toward the conduit rim. Indeed, Mode I fracture arrays may prove necessary for dissipating gas overpressures in the central regions of the magma column, which are considered difficult to outgas. These experiments highlight mechanisms that are likely active along conduit margins and constrain previously postulated processes under truly applicable conditions.

© 2016 Elsevier B.V. All rights reserved.

1. Introduction

The ease of gas escape from a volcanic system exerts a fundamental control on eruption style (Eichelberger et al., 1986; Woods and Koyaguchi, 1994). The effusion of silicic magmas occurs when magma is efficiently outgassed, curbing overpressure development and avoiding magma fragmentation, whereas, explosive eruptions and attendant fragmentation occur, in part, when magma is unable to sustain the shear stresses to which it is exposed. Thus, the conditions under which permeability develops within a rising and, therefore, deforming magma column are also conditions under which gas overpressure development and explosive behaviour may be avoided.

Porosity in magmas initially develops from decompression – (Sparks, 1978) and thermally-induced (Lavallée et al., 2015) vesiculation of isolated, pressurized bubbles, which supply the buoy-

ant forces necessary to drive magma upward. Ultimately, gas can only escape through a connected porosity network that eventually leads to the surface. To do this, the isolated bubble structure must be modified and become connected by expansion- (Burgisser and Gardner, 2004) and shear-induced bubble coalescence (Okumura et al., 2008) and/or magma rupture (e.g. Stasiuk et al., 1996). These gases then need to make use of pre-existing permeable networks, like those found in edifice- and dome-forming rocks (e.g. Eichelberger et al., 1986; Woods and Koyaguchi, 1994) or, when these escape routes are insufficient, by magma fragmentation (e.g. Kennedy et al., 2005). This interconnected void space can be created over time (Martel and Iacono-Marziano, 2015), often periodically (Tuffen et al., 2003), and subsequently destroyed (Rust and Cashman, 2004), making permeability in volcanic systems difficult to constrain.

When confronted with exceedingly high strain rates, magma is eventually susceptible to fracture (Webb and Dingwell, 1990b). Shear fractures near conduit edges facilitate gas escape by locally increasing permeability (Gaunt et al., 2014) and are preserved as ash-filled shear and extension fractures (commonly referred to

* Corresponding author.

E-mail address: alexandra.kushnir@gmail.com (A.R.L. Kushnir).

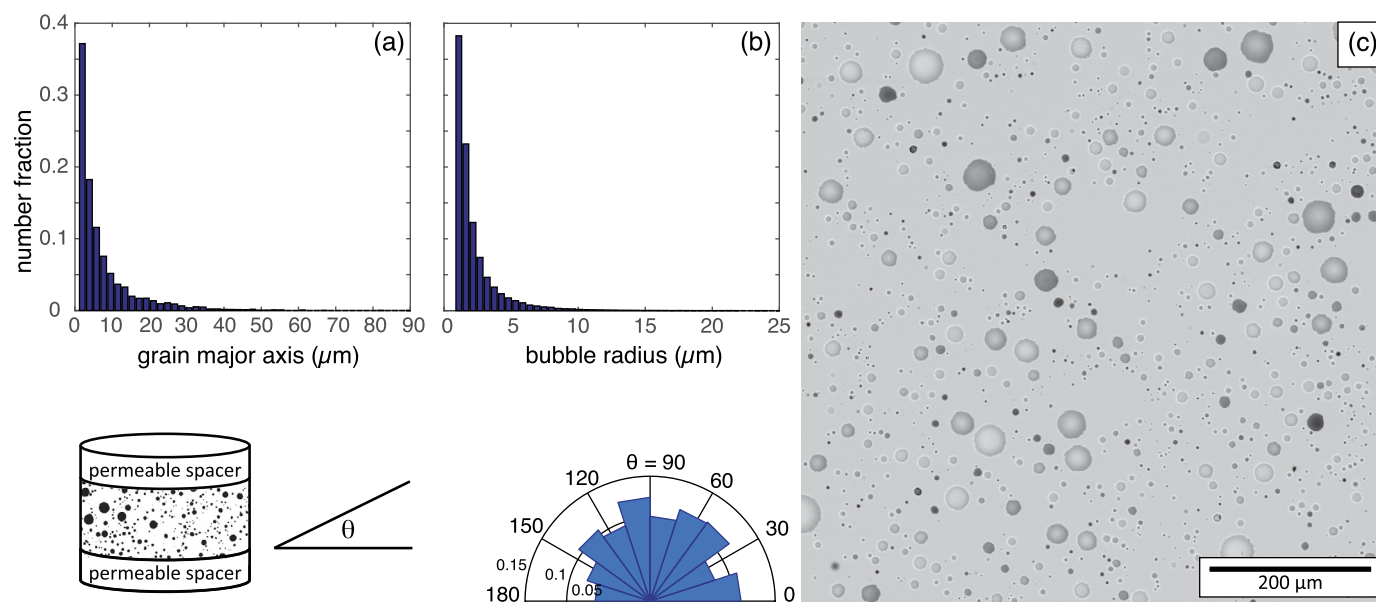


Fig. 1. Starting material. **(a)** 2D grain size distribution for the starting HPG8 powder. We defined the grain size by the length of the longest axis of the powder grains. The powder grain size is $<90\ \mu\text{m}$, with a dominant grain size of $2\ \mu\text{m}$. **(b)** 2D bubble radius distribution for the synthesized bubble-bearing magma. The polydisperse bubbles have a maximum and peak radius of $25\ \mu\text{m}$ and $2\ \mu\text{m}$, respectively. **(c)** SEM image of PP506, after synthesis. The rose diagram gives the orientations, θ , of the semi-major axes of the bubbles in the starting material, where θ is angle between the bubble semi-major axis and the shear zone boundary (the permeable spacer interface). Bubble/grain size distributions and orientations were determined by image analysis (using ImageJ) of SEM images. We note that, assuming the argon pore fluid behaves as an ideal gas under the experimental conditions described in the text, the isobaric decompression of the samples led to a 4-fold increase in total porosity and an increase in bubble radius by a factor of 1.6.

as tuffsite veins; e.g. Stasiuk et al., 1996; Tuffen et al., 2003; Castro et al., 2012). These fractures act as efficient transport networks for fluid flow, though repeated fracture events may be necessary to maintain permeability (e.g. Tuffen and Dingwell, 2005; Castro et al., 2012; Shields et al., 2016). Indeed, low-frequency earthquakes at conduit margins suggest that the occurrence of such fracture events is not unusual (e.g. Goto, 1999; Tuffen et al., 2003; Thomas and Neuberg, 2012). Unfortunately, shear-induced deformation along conduit walls may be relatively inefficient at outgassing the conduit centre (e.g. Castro et al., 2012; Gaunt et al., 2014) and strain localization along shear fractures may even limit further outgassing, eventually shutting off the permeable network lining the conduit rim (Okumura et al., 2010).

Several experimental studies have investigated permeability development as magma is deformed in simple shear. Permeability development facilitated by shear-induced bubble coalescence in magmas with moderate to high bubble fractions (>0.20) has been demonstrated experimentally (e.g. Okumura et al., 2008). At low bubble fraction (<0.20), crystal-assisted strain localization can result in bubble coalescence, locally increasing strain rates and inciting cataclastic behaviour that produces Riedel shear geometries (Laumonier et al., 2011). While shear-induced bubble coalescence and outgassing have been inferred in bubble-bearing phonolites containing less than 0.02 bubble fraction (Caricchi et al., 2011), outgassing in two- and three-phase magmas with low bubble fractions (<0.20) appears to be most efficiently facilitated by the development of helical shear fractures (Cordonnier et al., 2012; Shields et al., 2014). Shields et al. (2014) demonstrated that these helical fractures were composed of extension fractures (otherwise termed tensions gashes) oriented approximately perpendicular to the shear direction. Significantly, in the majority of these studies, gas escape was inferred postmortem (that is, post-experiment) by an overall reduction in bubble content (Pistone et al., 2012; Shields et al., 2014) and dissolved volatiles in the melt phase (Shields et al., 2014), making it difficult to identify when and by what mechanisms permeability developed. In particular, sample-

scale permeability development in shearing viscous flow via fracture development has not yet been confirmed *in situ*.

The purpose of this study is to begin to experimentally constrain permeability-producing processes previously postulated to be active at conduit margins. We demonstrate the mechanisms by which permeability develops in rhyolitic magmas of relatively low bubble fraction under conditions pertinent to volcanic conduits. We characterize permeability development *in situ* during simple shear of an initially impermeable, haplogranitic, two-phase (bubble and melt) magma as a function of shear strain rate. Further, we associate permeability development with microstructure to identify what mechanisms may influence volcanic behaviour in a natural setting.

2. Methods

Bubble-bearing magma analogues were synthesized and deformed in simple shear using an internally heated, gas-medium (argon) Paterson deformation apparatus equipped with a torsion motor and pore fluid pressure system (Paterson and Olgaard, 2000; Australian Scientific Instruments Pty Ltd; at ISTO, Orléans, France). Each experiment was performed in two steps: i) sample synthesis and ii) sample deformation, detailed below.

2.1. Starting material synthesis

To achieve a homogeneous, reproducible, bubble-bearing magma, we synthesized each sample prior to deformation. The anhydrous silicate melt had an haplogranitic composition (HPG8; prepared by Schott AG, Germany; see Supplementary Material for composition) and was chosen because it is rheologically well-characterized (Hess et al., 2001) and, as the eutectic composition of the quartz–albite–orthoclase system (Holtz et al., 1992), can be deformed at relatively low temperature without crystallisation perturbing its rheology. The HPG8 glass was ground in an agate mechanical grinder and sieved to below $90\ \mu\text{m}$; this polydisperse powder had a dominant grain length of $2\ \mu\text{m}$ (determined by image analysis, see below for details; Fig. 1A). For each experiment,

Download English Version:

<https://daneshyari.com/en/article/5780026>

Download Persian Version:

<https://daneshyari.com/article/5780026>

[Daneshyari.com](https://daneshyari.com)